MSc in Photonics

PHOTONICS**BCN**

Universitat Politècnica de Catalunya (UPC)
Universitat Autònoma de Barcelona (UAB)
Universitat de Barcelona (UB)
Institut de Ciències Fotòniques (ICFO)

http://www.photonicsbcn.eu

Master in Photonics

MASTER THESIS WORK

CASCADED CONICAL REFRACTION

Alejandro Turpin Avilés

Supervised by Dr. Jordi Mompart and Dr. Todor Kirilov (UAB)

Presented on date 12th July 2011

Registered at

Escola Tècnica Superior d'Enginyeria de Telecomunicació de Barcelona

Cascaded Conical Refraction

Alejandro Turpin Avilés

Grup d'Òptica, Dept. de Física, Universitat Autònoma de Barcelona, E-08193 Bellaterra, Spain

E-mail: alejandro.turpin@uab.cat

Abstract. After a brief introduction to the conical refraction phenomenon, the formation of transverse intensity patterns by a cascade of biaxial crystals with aligned optic axes is studied in detail. Up to 2^{N-1} concentric rings appear when a light beam passes through a system formed by N biaxial crystals with aligned optic axes. This fact is demonstrated experimentally with up to three crystals and a theoretical formulation of the phenomena is also provided. The theoretical method is based on the experimentally derived transformation rules for spatially filtered light beams propagating along the optic axis of a biaxial crystal. The experimental results are in full agreement with the theoretical predictions and the simplicity of the proposed theoretical method makes it very useful for calculating the intensity patterns of light beams propagating through an arbitrary set of aligned biaxial crystals.

Keywords: double refraction, conical refraction, biaxial crystals

1. Introduction to Conical Refraction

Double refraction, i.e., the decomposition of a ray of light into the ordinary ray and the extraordinary ray when it passes through an anisotropic crystal, was firstly discovered experimentally with a calcite crystal by Bartholin in 1669 [1] and explained within the wave theory by Huygens in 1690 [2]. Conical refraction (CR) is a relatively younger phenomenon that was firstly predicted by Hamilton in 1832 from Fresnel theory of light propagation in birefringent crystals and observed by Lloyd soon afterwards [3]. In CR, when a collimated light beam passes along the optic axis of a biaxial crystal it propagates inside the crystal in such a way that emerges from it giving rise to the characteristic transverse annular intensity pattern known as the CR ring; see figure 1(a). An exact diffractive solution of CR has been found only recently by Belsky and Khapalyuk [4] and later on extended by Belsky and Stepanov [5]. An elegant mathematical reformulation of this solution was recently performed by Berry [6].

The complete CR ring intensity pattern appears for both natural (unpolarized) light and for circularly polarized input light, see figure 1(c), being the intensity distribution uniform along the ring while if the input light beam is linearly polarized the intensity along the ring forms a crescent pattern; see figure 1(d). Moreover, every two diagonally opposite points of the CR ring are orthogonally linearly polarized and the polarization distribution does not depend on the polarization state of the incident beam. On the other hand, in experimental situations it is common to focus the laser beam into the crystal with a lens. In this case, as the observation plane is moved, a transition from what is known as Raman spot [7] to secondary rings of CR and then to the characteristic CR ring pattern (that appears at the so-called Lloyd plane) is observed, as it appears in figure 2. A last relevant characteristic is that at the Lloyd plane there two rings with different intensities separated by a dark ring called as

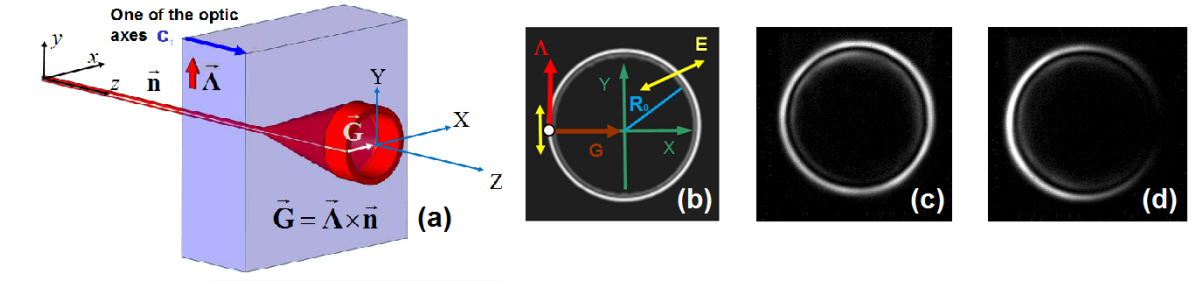

Figure 1. (a) Generation of the CR ring as an input Gaussian light beam propagates along the optic axis of a biaxial crystal with characteristic Λ-vector; $\vec{G}$ is the displacement that suffers the beam when passes through the crystal and characterized by $\vec{G} = [\vec{\Lambda} \times \vec{n}]$. (b) Ring intensity pattern at the Lloyd plane (the input light beam is represented by closed white circle) and scheme of the characteristic vectors and notation. (c) Ring intensity pattern for circularly polarized light. (d) Crescent intensity pattern for vertically linearly polarized light. Figures (b) - (d) are experimental results.

the Poggendorff dark ring in honor of its discoverer as it can be seen in figure 1(c) with the splitting between the two rings.

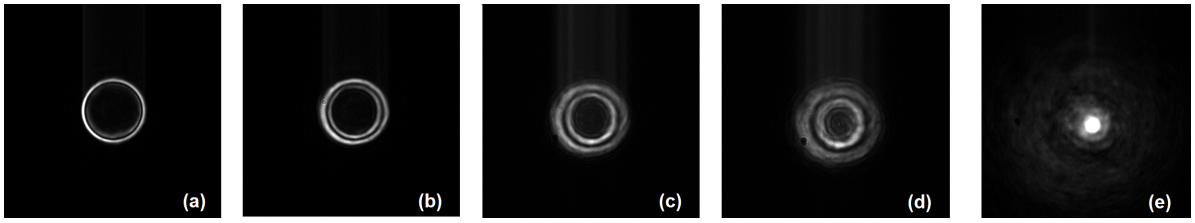

Figure 2. Experimental images that show the evolution of the CR pattern from the Lloyd plane (a) until the Raman spot (e). It can be clearly seen the intermediate steps of secondary rings (b) - (d).

Regarding the experimental works, the number of studies done in this field are not many, at least until the last five years, when the fashion for the phenomenon has grown. The first one in analyse experimentally CR was Lloyd [3] in 1832 and, seven years later, Poggendorff [8] discovered the splitting between the two rings. This fact was partially explained by Voigt [9] in 1905. The following experimental contribution in the field was done by Raman in 1942 [7], who realized that if the observation plane is moved the CR ring disappears and almost all the light gets concentrated in the center of the ring, as shown in figure 2(e). Qualitative works of CR phenomena can be found in Perkalskis & Mikhailichenko (1979) [10] and also quantitative comparisons with theory in Schell & Bloembergen (1978) [11], Féve *et al* (1994) [12] and, more recently, in Kalkandjiev & Bursukova (2008) [13] and Abdolvand (2011) [14]. On the other hand, most of the authors distinguish between internal and external CR and this fact leads to some confusion (see [15] for instance). This confusion arises when one tries to use geometrical optics to explain and understand CR. Actually, using diffractive optics theory only one type of CR refraction (internal), when light propagates along the wave optic axis of a biaxial crystal, has been predicted [16].

Another phenomenon that has only recently been studied theoretically is cascaded CR [17]. The aim of the present work is to study both experimentally and theoretically (from simulations) cascaded CR with up to three crystals, since it is an interesting and not well known phenomenon that can have potential applications in image processing and laser techniques. The analysis will be based on the

transformation rules deduced by Loiko *et al* [18] when filtered beams are used. A CR-filtered beam is defined as a beam that is obtained when a pinhole is placed at some point of the CR ring, so that it is a linearly polarized beam. In section 2 cascaded CR will be shown in general, without using CR-filtered beams. In section 3, CR-filtered beams will be generated at the first crystal (CRE_1) and then we make them propagate through the other two crystals (CRE_2 and CRE_3). Theoretical basis of the phenomena and simulations of the experimental results are also shown in the same section. Finally, in section 4, conclusions and results of the paper are summarized.

2. Cascaded conical refraction: an experimental approach

As it has been indicated in the Introduction, the most characteristic feature of CR is the ring pattern. In previous experiments Kalkandjiev & Bursukova [13] have shown that a Gaussian beam passed through two CREs splits into two rings at the Lloyd plane. Moreover, they have predicted the emergence of 2^{N-1} concentric rings (each of which is split by the Poggendorff dark ring) for a cascade of N biaxial crystals. Berry [17] has performed exhaustive theoretical studies on cascaded CR. In the present work, theoretical insight into the pattern formation of multiple rings in cascaded CR is presented and experimentally studied and verified with up to $N = 3$ crystals by using the experimental setup shown in figure 3.

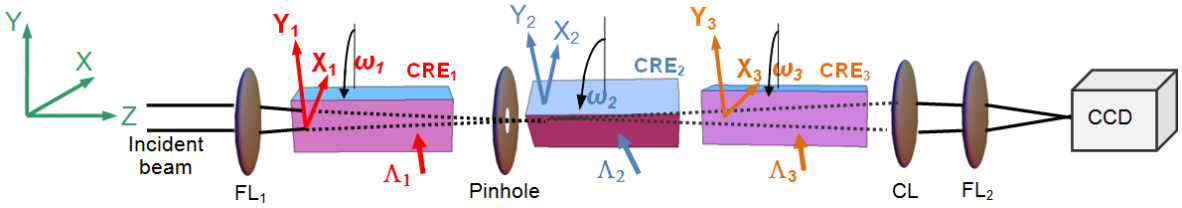

Figure 3. General setup for the experiments. A collimated incident beam is focused by means of a focusing lens (FL_1) and passed along the optic axes of the three crystals (CRE_1, CRE_2, CRE_3). Then, light is collimated again (CL) and imaged (FL_2) in the CCD camera. The incident beam can be either circularly or linearly polarized and crystals have their own orientation of their $\vec{\Lambda}$ [13], given by the angle of rotation ω_i. The effect of inserting a pinhole is considered in the experiments of section 3. Along the experiment, lenses with dielectric coating and focal lenghts of 100mm, 150mm and 200mm are used.

The laser beam coming from a diode laser pigtailed to a monomode fiber has Gaussian profile with waist radius of $w = 1.5$ mm and wavelength of 640 nm. The crystals used here ($Nd:KGd(WO_4)_2$) have been provided by Conerefringent Optics SL and their general characteristics can be found in Table 1. The action of these crystals over the light can be characterized by the lateral shift $\vec{G}$ of the emerging ring. Therefore, some material tensor inducing $\vec{G}$ should be fixed to the CRE and this is the $\Lambda-$vector ($\vec{\Lambda}$). The existence of $\vec{\Lambda}$ can be deduced from the ray theory and can be shown that it accomplishes the relation $\vec{G} = \vec{\Lambda} \times \vec{n}$ (so that, $|\vec{\Lambda}| = |\vec{G}|$), where $\vec{n}$ is the direction of propagation of the input beam; see figure 1(a). Moreover $\vec{\Lambda}$ contains information about the length of the crystal and its amplitude can be measured by the ring radius $R_0 = |\vec{G}|$ at the Lloyd plane (consequently, the Λ-parameter that appears in Table 1 is just the modulus of $\vec{\Lambda}$ and is the value of the ring radius). Moreover, along the experiment, crystals have not been in contact but they are wide enough in order to allow each pattern to enter fully into the next crystal. Finally, regarding the CCD sensor, it is a Sony-IXI095 with resolution of 1360×1024 pixels and a pixel size of 6.5 μm^2.

There are many different experimental configurations in order to analyse cascaded CR but our starting point will be firstly consider two identical crystals with both the same and arbitrary orientation of their $\vec{\Lambda}$ (the ring pattern obtained for each of the crystals is shown in figure 4). When both $\vec{\Lambda}$ of

Table 1. Parameters of the crystals used in the experiments

	CRE_1	CRE_2	CRE_3
Λ – parameter(μm)	397	311	181
Length (L_i)(mm)	23.38	18.30	10.62
Cross section (mm^2)	21.78	21.76	23.72
Angular misalignment (mrad)	≤ 1.25	≤ 1.25	≤ 1.25

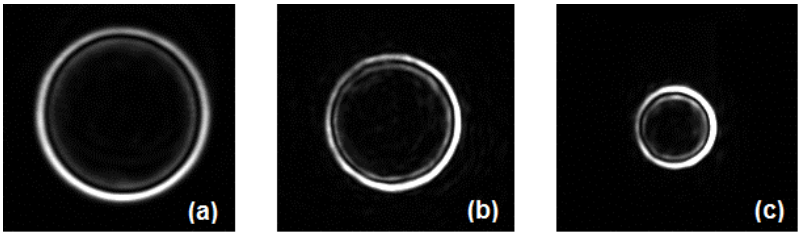

Figure 4. Experimental images about CR rings of the different crystals CRE_1(a), (b) and CRE_3(c) used in the present work. The charasteristic parameters of the crystals are shown in Table 1.

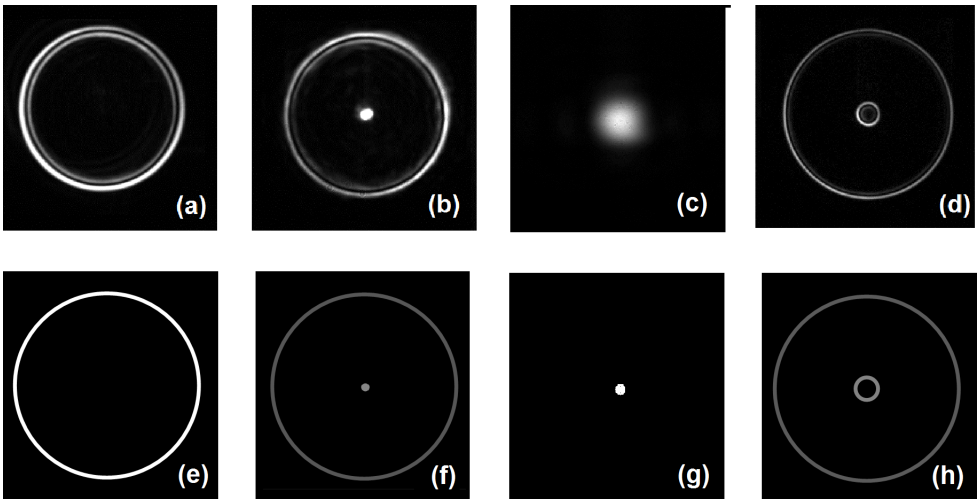

Figure 5. Transverse light intensity patterns at the Lloyd plane for a cascade of two crystals with the same lengths ($L_1 = L_2 = 23.38$ mm) and with: (a) $\omega_2 - \omega_1 = 0^o$ (parallel $\vec{\Lambda}$); (b) $\omega_2 - \omega_1 = 90^o$; (c) $\omega_2 - \omega_1 = 180^o$ (antiparallel $\vec{\Lambda}$). (d) shows cascaded CR for two crystals ($L_1 = 23.38$mm, $L_2 = 18.30$ mm) with $\omega_2 - \omega_1 = 45^o$. In figures (b) and (d) the angle of rotation of the crystals has been optimised in order to obtain the same intensity both for the ring and the point and for the two rings respectively. (e) - (h) are simulations of the corresponding experimental images (a) - (d) obtained using the formulation given in sections 3.3 and 3.4.

the crystals are parallel, the resulting pattern is the same to that one expected with only one crystal of length $L = L_1 + L_2$ and this fact is in complete agreement with the theory (figure 5(a)). Moreover, in this particular case, since the crystals have the same $\vec{\Lambda}$, when we rotate one of the crystals we don't obtain a pair of concentric rings but a ring with a spot in the center; see figure 5(b). Another

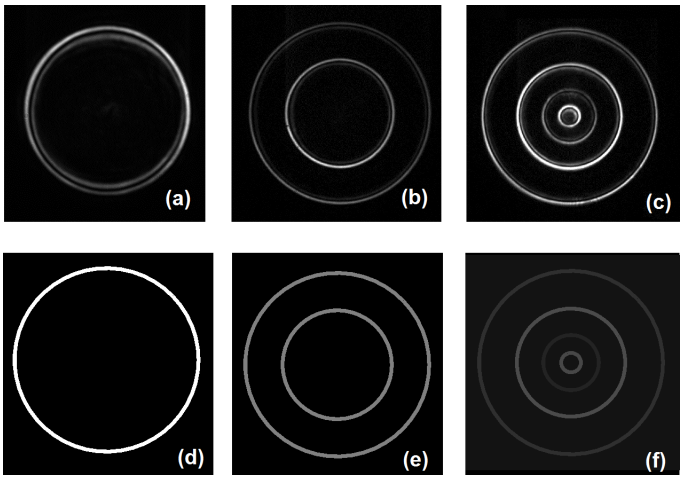

Figure 6. Transverse light intensity patterns at the Lloyd plane for cascaded CR using three crystals with lengths $L_1 = 23.38$mm, $L_2 = 18.30$ mm and $L_3 = 10.62$mm. $\omega_1 = \omega_2 = \omega_3 = 0^o$ (a). $\omega_1 = \omega_2 = 0$, $\omega_3 = 90^o$ (b) and (c) is one example of the most general case, being $\omega_1 = 0^o$, $\omega_2 = 45^o$ and $\omega_3 = 135^o$. (d)-(f) are simulations of the corresponding phenomena of experimental images (a)-(c) obtained using the formulation given in sections 3.3 and 3.4.

interesting phenomenon is the pattern obtained when the two identical crystals are placed with opposite orientations, i.e., $\vec{\Lambda}_1 = -\vec{\Lambda}_2$. In this case the crystals counteract each other action over the light and the initial beam is restored if they are perfectly adjusted, as it can be seen figure 5(c). If two different crystals are placed and ω_1 and ω_2 are different, there appears the most general pattern consisting in two concentric rings; see figure 5(d). An interpretation of all these patterns will be given in next section.

Now, if we introduce a third crystal and all the crystals are identically oriented ($\omega_1 = \omega_2 = \omega_3$), the resulting pattern will be analogous to the case with two crystals, i.e., only one ring whose radius is related to a crystal with length $L = L_1 + L_2 + L_3$ will be generated, as figure 6(a) shows. However, if we put two crystals with the same orientation and the CRE_3 with a different one, the emerging pattern from the system consists in two concentric rings (see figures 6(b) and (c)), which is similar to the case of two different cristals shown in figure 5(c). In figure 6(c) it can be found the most interesting phenomenon, that is produced when the three CREs are oriented at different angles in which case a pattern of four rings is formed in general.

3. Cascaded conical refraction with CR-filtered beams

3.1. CR-filtered beams and their characteristics

Recently, it has been shown [18] that with a properly located pinhole at the Lloyd plane, one can filter a part of the CR ring, i.e., a part of the input Gaussian beam. In what follows such beam will be called as the CR-filtered beam. This beam can be characterized by the plane of the electric field vector $\vec{E}$ and by the value of the angle ϕ, at which it has been filtered, as shown in figure 7. The latter property can be equivalently described by the vectors $\vec{\Lambda}$ or $\vec{G}$ of the CRE through which this beam has passed. It has to be mentioned that the vector $\vec{\Lambda}$ and the angle ϕ are intrinsical characteristics of the CR−filtered beam after the filtering procedure. In the fixed (non rotated) laboratory reference system of coordinates we introduce the angles ω and $\theta = \omega - \pi/2$ to describe orientation of the vectors $\vec{\Lambda}$ and $\vec{G}$, respectively, and the azimuth Φ for the plane of linearly polarized electric field vector $\vec{E}$. These

angles are interrelated as follows

$$2(\Phi - \theta) = \phi, \tag{1}$$

$$2(\Phi - \omega) = \phi - \pi. \tag{2}$$

From now on symbol ϕ (with subscripts) will be used to denote the parameter of the CR−filtered beam in the reference frame associated with CRE, through which this filtered beam has passed. Therefore, any CR−filtered beam can be equivalently described by any of the following combinations $[\phi, \omega]$, $[\phi, \theta]$, $[\Phi, \omega]$ or $[\Phi, \theta]$, or with the corresponding vectors: $[\vec{E}, \vec{\Lambda}]$ or $[\vec{E}, \vec{G}]$.

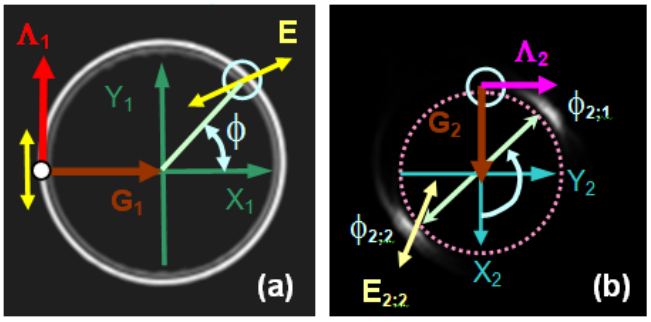

Figure 7. Spatial filtering in CR and transformation rules for the CR filtered beams. (a) $[\phi, \omega]$−filtered beam is produced by placing a pinhole (represented by small open circle) at an angle ϕ of the CR ring. (b) Two refracted beams $[\phi_{2;1,2}, \omega_2]$ into which the $[\phi, \omega]$−filtered beam of (a) splits when it passes through a biaxial crystal (CRE_2) with characteristic vector $\vec{\Lambda}_2$ rotated by an angle ω_2. Dashed circle in figure (b) represents schematically the ring pattern expected under CR of the input fundamental Gaussian beam. Open circle represents the position of the $[\phi, \omega]$−filtered beam in (a). Yellow double arrows in both figures denote the polarization planes of the electric field vectors at corresponding points.

3.2. Transformation rules for CR-filtered beams

We consider transformation of a CR filtered beam $[\phi, \omega]$ passed along the optic axis of a biaxial crystal. For this purpose the setup of figure 3 was carried out but with the CRE_3 being removed. $[\phi, \omega]$−filtered beam is produced by placing a pinhole at an angle ϕ at the Lloyd plane of the first crystal rotated by an angle ω_1 as shown in figure 7. Loiko *et al* observed [18] that when a CR−filtered beam passes through a CRE, for instance, through the second crystal (CRE_2) of our setup, it does not produce the characteristic ring intensity pattern. Instead, in the general case, it splits (refracts) into two beams with orthogonal linear polarizations that correspond to the two opposite points of the otherwise expected ring of CR. In figure 7(b) this expected CR ring is shown by the dashed circle. When the CRE_2 with characteristic vector $\vec{\Lambda}_2$ is rotated by an arbitrary angle ω_2 around the beam propagation direction, the characteristic angles of the two refracted beams $\phi_{2,1}$, $\phi_{2,2}$ measured in the reference coordinate system X_2Y_2 of the CRE_2 (see figure 7(b)) and their intensities $(I_{2,1})$, $(I_{2,2})$ are varied in accordance to the following transformation rules deduced in [18]:

$$I_{2,1} = I\cos^2\left(\frac{\omega_1 - \omega_2}{2}\right),\ I_{2,2} = I\sin^2\left(\frac{\omega_1 - \omega_2}{2}\right), \tag{3}$$

$$\phi_{2,1} = \phi - (\omega_2 - \omega_1),\ \phi_{2,2} = \phi_{2,1} + \pi, \tag{4}$$

where $I = I_{2,1} + I_{2,2}$ denotes the total energy of the input $[\phi, \omega]$−filtered beam. In figure 8(b) we present an experimental example on transformation of the CR−filtered beam [$\phi = 0^o$,$\phi = 180^o$;

$\omega_1 = 90^o$] by a biaxial crystal CRE_2 with the $\vec{\Lambda}_2$ orientated at $\omega_2 = 0^o$. The two refracted beams are [$\phi^+_{2,1} = 0^o$,$\phi^+_{2,2} = 180^o$; $\omega_2 = 0^o$] and [$\phi^-_{2,1} = 180^o$,$\phi^-_{2,2} = 360^o$; $\omega_2 = 0^o$]. It has to be also noted that the refracted beams obtained with any CRE are also CR-filtered beams, so that if one of the two beams is selected and allowed to pass through another CRE it will refract into two beams obeying the transformation rules (3, 4). Therefore, these rules can be consecutively applied to find transverse patterns for light beams passed along optic axes of multiple biaxial crystals and this is the fundamental subject of this work on this section.

3.3. Refraction in two biaxial crystals using CR-filtered beams description

The experimental setup is shown in figure 3 but with the CRE_3 being removed. In cascaded CR, the energies distributed in the pattern of the rings depend on the relative orientation of the $\vec{\Lambda}$ of each CRE, and they obey the law (3). Here it is explained how such intensity pattern appears and how it relates to the CR-filtered beams introduced previously. The first crystal (CRE_1) makes decomposition of the input Gaussian beam into the CR-filtered beams with continuously varying parameter ϕ. In the absence of the CRE_2 they provide usual ring intensity pattern at the Lloyd plane. In this case, the spatial positions of the $\phi-$filtered beam on the CR ring, are given as follows

$$\vec{\rho}(\phi) = \vec{\rho}_0 + \vec{G_1} + |\vec{G_1}| \cdot \left[\cos(\phi \pm \omega_1 - \frac{\pi}{2}), \sin(\phi \pm \omega_1 - \frac{\pi}{2})\right], \tag{5}$$

where $\vec{\rho}_0$ is the position of the incident light beam. The CRE_2 splits any CR-filtered beam passed along it optic axis into two ones obeying the transformation rules (3, 4). With two CREs of relative orientation given by $\omega_2 - \omega_1 = 45^o$, the splitting procedure is demonstrated theoretically in figure 8(c) and experimental results are shown in figure 8(a) for two CR$-$filtered beams after the CRE_1 at angles $\phi = 0^o$ and $\phi = 180^o$. For an input CR-filtered beam centered at $\vec{\rho}_0$ the transverse positions of the two refracted beams after the CRE_2 in the fixed (laboratory) system of spatial coordinates can be calculated as follows

$$\vec{\rho_\pm}(\phi_{2;1,2}) = \vec{\rho}(\phi) + \vec{G_2} + |\vec{G_2}| \cdot \left[\cos(\phi_2 \pm \omega_1 - \frac{\pi}{2}), \sin(\phi_2 \pm \omega_1 - \frac{\pi}{2})\right]. \tag{6}$$

By doing such calculations for all CR$-$filtered beams with continuously varying parameter ϕ in the range [0, 2π], one obtains two sets of the refracted CR-filtered beams with continuously varying parameters $\phi_{2,1}$ and $\phi_{2,2}$ (defined by the equation (4)) both in the range [0, 2π]. The energies of the two rings are described by (4), while their radii are defined by the expression:

$$R_2^\pm = |\vec{\rho}(\phi_{2;1,2}) - \vec{\rho}_c| = \left||\vec{G_1}\| \pm |\vec{G_2}|\right|, \tag{7}$$

with $\vec{\rho}_c = \vec{\rho}_0 + \vec{G_1} + \vec{G_2}$ being the position of ring's centre. The analytical results shown in figure 8(c) and figure 8(d) reproduces well the experimental ones shown in figures 8(a) and (b), so that as the theory developed in [18] by Loiko *et al* affirms, after the filtering process, no ring appears but four points for each CR-filtered beam (in our case we have lines instead of points because of the diffraction at the CR-filtered beam). The asymmetries in the intensity profile are due to the possible imperfections in the adjustment of the crystals, the aberrations of the optics used and the position of the filtering mechanism with respect to the Lloyd plane. It has been checked that for any orientation of the biaxial crystals, i.e., for any combination of the CREs defined by the vectors $\vec{\Lambda}_i$, this analytical approach reproduces well the position of the rings and their intensities observed in previous experiments [13].

3.4. Refraction in three and N biaxial crystals

Now we consider a case when the third crystal (CRE_3) with the characteristic vector $\vec{\Lambda}_3$ is added after the first two crystals (CRE_1 and CRE_2), i.e., we consider complete setup shown in figure 3. Previously it has been shown that with a pinhole positioned on the CR ring after the CRE_1, two CR-filtered beams appear after the CRE_2. The CRE_3 further splits each of these filtered beams into two ones; as a

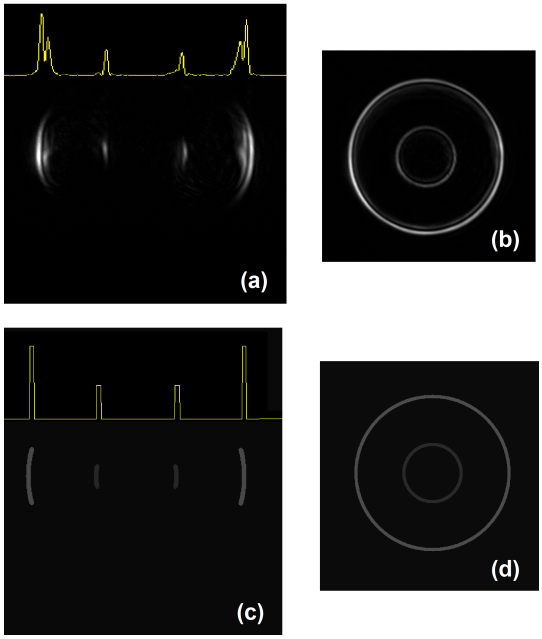

Figure 8. Transverse light intensity patterns at the Lloyd plane for cascaded CR using two crystals with lengths $L_1 = 23.38$mm, $L_2 = 18.30$ with $\omega_1 = 0^o$ and $\omega_2 = 45^o$ and beams filetered at $\phi = 0$ and $\phi = \pi$ by means of a slit with an aperture of 21μm.(a) and (b) show the experimental result after and before filtering, respectively. (c) and (d) are simulations of experimental images (a) and (b) obtained using the formulation given in sections 3.3 and 3.4. The intensity profiles along the horizontal direction at the center of the image can be found in yellow.

result, four CR-filtered beams appear after the CRE_3 as it is shown in figure 9(a) (experimentally) and figure 9(c) (theoretically). By doing the same simulations for the CR-filtered beams with parameters $\phi_{2,1}$ and $\phi_{2,2}$ (see equation (6)) continuously varying in the range $[0,\ 2\pi]$ for inner and outer rings, that are produced by the CRE_1 and CRE_2, one obtains four rings as shown in figure 9(d). The CR filtered beams belonging to these four rings can be obtained by applying equation (6) replacing $\vec{\rho}(\phi)$ by $\vec{\rho_{\pm}}(\phi_{2;1,2})$, ϕ by $\phi_{2;1}$ and $\phi_{2;2}$ and with $\vec{G}_2$ being replaced by $\vec{G}_3$, in addition to the transformations rules (3, 4). Therefore, the third crystal shifts the position of the rings centre to a new position given by the vector $\vec{\rho}_c = \vec{\rho}_0 + \vec{G_1} + \vec{G}_2 + \vec{G}_3$ and it splits each of the two (inner and outer) rings emerging after the second crystal ($R_2^{\pm}$) into two new ones with the radii given by:

$$R_3^{\pm;\pm} = \left| R_2^{\pm} \pm \|\vec{G}_3| \right|, \tag{8}$$

where $\pm;\pm$ specifies that there can be four different rings corresponding to all the possible combinations $\{++, +-, -+, --\}$. Theoretically estimated pattern of the four rings obtained on the basis of the transformation rule (3) and the equation (8) is shown in figure 9(d), which reproduces well the experimentally observed results shown in figure 9(b). The results obtained here can be generalized to the case of N CREs considering that a set of N CREs with characteristics vectors $[\vec{\Lambda}, \vec{G}]$ splits an input beam of Gaussian transverse profile into 2^{N-1} rings with radii given by 2^{N-1} possible combinations of coefficients q_n^k equal to either $+1$ or 1:

$$R^{(k)} = |\vec{G_1}| + \sum_{n=2}^{N} q_n^{(k)} |\vec{G}_n|, \tag{9}$$

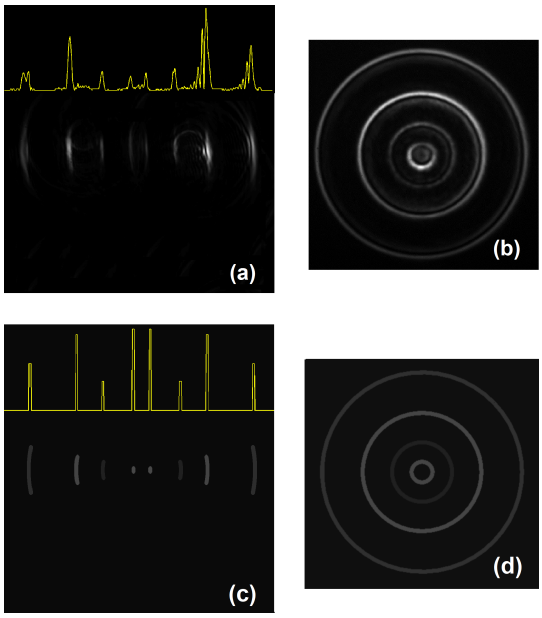

Figure 9. Light pattern at the Lloyd plane for cascaded CR under the same configuration as in figure 6(c, f) and beams filetered at $\phi = 0$ and $\phi = \pi$ by means of a slit with an aperture of 21μm. (a) and (b) show the experimental result after and before filtering respectively. (c) and (d) are simulations of the corresponding phenomena of experimental images (a) and (b) obtained using the formulation given in sections 3.3 and 3.4. The intensity profiles along the horizontal direction at the center of the image can be found in yellow.

and provides a lateral shift for the centre of the input beam from the position ρ_0 to the new position ρ_c. At the Lloyd plane this shift is given by the vector

$$\vec{\rho_c} = \vec{\rho_0} + \sum_{n=1}^{N} \vec{G}_n, \tag{10}$$

The positions of the points along the k-th ring can be described by the following vectors

$$\vec{\rho}^{(k)} = \vec{\rho_c} + R^{(k)} \cdot \vec{u}_{\vec{G}_{\text{tot}}}, \tag{11}$$

where $\vec{u}_{\vec{G}_{\text{tot}}}$ is an unitary vector in the direction given by $\left[\cos(\phi_N \pm \omega_{N-1} - \frac{\pi}{2}), \sin(\phi_N \pm \omega_{N-1} - \frac{\pi}{2})\right]$ with ϕ_{N-1} and ϕ_N being computed recursively using (4) with parameter ϕ is varied in the range $[0, 2\pi]$. For an unpolarized, randomly or circularly polarized input beam with fundamental Gaussian transverse profile, the rings have uniform intensity distribution along the patterns. The energy or power of each ring could be determined by successively applying equation (3).

4. Conclusions

Being a nontrivial phenomenon with a complex solution, here cascaded CR with up to three crystals has been experimentally studied and presented using a theoretical approach based on the experimentally derived rules for the refraction and splitting of spatially filtered light beams propagated along an optic axis in biaxial crystals. Such filtering corresponds to the angular selection of a part of the CR ring. Under this approach, the first crystal separates the input Gaussian beam into a collectivity of CR−filtered beams with continuously varied characteristic parameter ϕ, which (in the absence of the

other consecutive crystals) provides the ring of CR usually observed with single biaxial crystal. The consecutive crystals split each of the CR−filtered beams into two ones. Therefore, the CR ring after the first crystal is split by the remained N-1 crystals into 2^{N-1} concentric rings. In all the studied cases the presented method fit the experimental results, proving its usefulness and accuracy in the computation of the position and the intensity of the emerged rings.

Acknowledgments

This research has been performed with the financial support given by the Spanish Ministry of Science and Innovation under contracts FIS2008-02425, FIS2010-10004-E and CSD2006-00019 (Consolider project "Quantum Optical Information Technologies"), and the Catalan Government under contract SGR2009-00347. I am indebted to my advisors, Prof. Mompart and Prof. Kalkandjiev and specially to Dr. Loiko for his help and encouragement throughout the course of this work. In addition I would also like to thank Mr. Benseny for his comments and suggestions.

References

[1] Bartholin, E. 1669 Experimenta crystalli islandici disdiaclastici: Quibus mira et insolita refractio detegitur *Hafniae*.
[2] Huygens, C. 1690 Trait de la lumire *Pieter van der Aa, Leiden, Netherlands*.
[3] O'Hara, J. G. 1982 The prediction and discovery of conical refraction by William Rowan Hamilton and Humphrey Lloyd *Proc. R. Ir. Acad.* 82 **2**, 231-257.
[4] Belskii, A. M. & Khapalyuk, A. P. 1978 Internal conical refraction of bounded light beams in biaxial crystals, *Opt. Spectrosc. (USSR)* **44**, 436439.
[5] Belsky, A. M. & Stepanov, M. A. 1999 Internal conical refraction of coherent light beams, *Opt. Commun.* **167**, 15.
[6] Berry, M. V. & Jeffrey M. R. 2007 Conical diffraction: Hamiltons diabolical point at the heart of crystal optics, *Prog. Opt.* **50**, 13-50.
[7] Raman, C. V. 1942 The phenomena of conical refraction, *Curr. Sci.* **11**, 4446.
[8] Poggendorff, J. C. (1839) Ueber die konische refraction, *Pogg. Ann.* **48**, 461462.
[9] Voigt, W. 1905a Bemerkung zur theorie der konischen refraktion, *Phys. Z.* **6**, 672673.
[10] Perkalskis B. S. and Mikhailichenko Y. P. 1979 Demonstration of conical refraction, *Izv Vyss Uch Zav Fiz* **8**,103105.
[11] Schell, A. J. & Bloembergen, N. 1978a Laser studies of internal conical diffraction. I. Quantitative comparison of experimental and theoretical conical intensity distribution in aragonite, *J. Opt. Soc. Am.* **68**, 10931098.
[12] Fève, J. P. **et al** 1994 Experimental study of internal and external conical refraction in KTP, *Opt. Commun.* **105**, 243252.
[13] Kalkandjiev T. K. & Bursukova, M. A. 2008 Conical refraction: an experimental introduction, *Proc. SPIE* **6994**.
[14] Abdolvand, A. 2011 Conical diffraction from a multi-crystal cascade: experimental observations, *Appl. Phys B* **103**, 281-283.
[15] Born, M. & Wolf, E. 1999 *Principles of optics (7th Ed.)* London: Pergamon Press.
[16] Belskii A. M. & Khapalyuk, A. P. 1978 Propagation of confined light beams along the beam axes (axes of single ray velocity) of biaxial crystals, *Opt. Spectrosc.* **44**, 312-315.
[17] Berry, M. V. 2010 Conical diffraction from an N-crystal cascade, *J. Opt.* **12** 075704.
[18] Loiko, Y. *et al* 2010 Fermionic transformation rules for spatially filtered light beams in conical refraction, *Proc. SPIE* 7950 **12**.